

# Mechanism of remote epitaxy using two dimensional materials

by

Samuel Cruz

B.S.M.E., Georgia Institute of Technology (2015)

SUBMITTED TO THE DEPARTMENT OF MECHANICAL ENGINEERING IN PARTIAL  
FULFILLMENT OF THE REQUIREMENTS FOR THE DEGREE OF

MASTER OF SCIENCE IN MECHANICAL ENGINEERING

AT THE

MASSACHUSETTS INSTITUTE OF TECHNOLOGY

JUNE 2017

© Massachusetts Institute of Technology 2017. All rights reserved.

Author: \_\_\_\_\_

**Signature redacted**

Department of Mechanical Engineering

Certified by: \_\_\_\_\_

**Signature redacted**

May 12, 2017

Jeehwan Kim

Class '47 Career Development Chair Assistant Professor

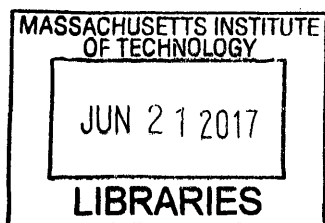
Thesis Supervisor

Accepted by: \_\_\_\_\_

**Signature redacted**

Rohan Abeyaratne

Quentin Berg Professor of Mechanics; Graduate Officer



ARCHIVES

This page is intentionally left blank

# Mechanism of remote epitaxy using two dimensional materials

by

Samuel S. Cruz

Submitted to the Department of Mechanical Engineering on May 12, 2017 in Partial Fulfillment of the Requirements for the Degree of Master of Science in Mechanical Engineering

## Abstract

Van der Waals epitaxy (vdWE) has gained great interest as it provides the ability to relax the strict lattice matching conditions required in conventional epitaxy of covalent or ionic single crystal substrates. With the rise of two-dimensional (2D) materials since the isolation of graphene in 2004, vdWE has been attempted on 2D materials, transferred, or grown on substrates. However, there has been the notion that the 2D material is the seed layer in van der Waals epitaxy. Notwithstanding, the substrate below the 2D material may play a role in orienting the crystalline growth of overlayers. This is supported by previous studies of a so called “long range” effect, where the potential field of growth substrates influenced the crystal orientation of overlayers through thin amorphous layers, and the “transparency” of graphene, where the contact angle of a droplet was unchanged by the presence of graphene. Here, we report the ability of the underlying substrate below graphene to assign the epitaxial registry of adatoms despite its presence, and thus form epitaxial layers with the same crystal orientation as the substrate during vdWE. Density functional theory (DFT) calculations are utilized to find that the critical separation gap beyond which a substrate and overlayer will lose electronic interaction is  $\sim 9 \text{ \AA}$ , which allows for the insertion of thin graphene at the substrate-epilayer interface. We experimentally test the interaction as a function of distance by transferring monolayer, bilayer and tetra-layer graphene onto GaAs (001) and performing homoepitaxial growth. The results show that single crystalline GaAs with (001) orientation is only obtained on monolayer graphene, revealing that only monolayer graphene may allow the substrate to have influence over the orientation of the overlayer. The method is applied to the homoepitaxial growth of GaP and InP with the same result. The findings further the development of the two-dimensional material based transfer (2DLT) technique, which permits the single crystalline growth of semiconductor materials on top of 2D materials followed by their release and transfer to desired substrates, allowing for novel device designs for applications in advanced and flexible electronics.

Thesis Supervisor: Jeehwan Kim

Title: Assistant Professor of Mechanical Engineering

Note: The work contained herein is based on a published work. See reference (1).

## Table of Contents

Abstract.....	3
Acknowledgements.....	5
List of Figures.....	7
Mechanism of Remote Epitaxy using Two Dimensional Materials .....	8
Background.....	8
The “long range” effect.....	8
The advent of van der Waals epitaxy.....	12
The emergence of graphene and 2D materials.....	13
Orienting contributions from the underlying substrates in vdWE using 2D materials.....	14
Our use of graphene.....	15
Gallium Nitride epitaxy on graphene.....	16
Research objectives.....	17
Epitaxial growth through graphene.....	19
Role of the underlying substrate in GaN/graphene/SiC system.....	19
Density functional theory simulations .....	21
Experimental trials of remote epitaxy.....	26
Probing remote epitaxy through other substrates.....	31
Conclusion .....	33
Future work.....	33
References.....	36

## Acknowledgements

I am foremost grateful to the reason I am who I am today, my motivation, the reason I have true life, and the reason I have learned how to love: to my Lord, my savior, Jesus Christ, and God, my Father. I did not know what true life was, until I believed in you, and received the great, promised gift of God (John 4:10).

I thank my adviser, Professor Jeehwan Kim, for his mentorship, friendliness, understanding character, and patience. I have learned a lot from you, and your motivation is contagious. Thank you for encouraging your students and inciting in us constant motivation and for a fun but tough several months. Also for directing the research which forms this work.

I also want to thank my lab group members, some of who are still at MIT, some of whom have left, but from whom I have received help one way or another. Thank you for your collaborating character. Among you are Yunjo Kim, Shinhyun Choi, Wei Kong, Ibraheem Almansouri, Scott Tan, Kuan Qiao, Kyusang Lee, Chanyeol Choi, Geng Zhi, and Jaewoo Shim. Special shout out to Yunjo Kim, whom I have very closely worked with since I began MIT.

There are several key people whom I would like to thank for carrying this research forward. Among them are Professor Eugene Fitzgerald's group in DMSE at MIT. Specifically, I would like to thank Christopher Heidelberger, Rushabh Shah, and Roger Qingfeng Jia for their help, assistance, support, friendship, patience, and training on the MOCVD. It has been fun and pleasant to work with all of you for the past several months at MIT, and I have learned a great amount from your experience in research.

I would like to acknowledge the excellent work of Professor Jinwoo Hwang, and his graduate student Jared M. Johnson, for working closely with us to produce excellent TEM images, some of which are included in this work. I also thank Professor Alexie Kolpak, and her graduate student, Babatunde Alawode, for working closely with us and providing very many insights with simulations regarding the experiments we wanted to conduct. Your collaboration has been key in the production of this work. To Professor Jing Kong in DMSE, and her graduate student Yi Song, I thank for their collaboration in helping us get started with graphene transfers when our group

recently began at MIT, and for all the great help your group has provided to many members of our research group.

And of course, I would like to thank my dear family, Ximena Chois, Hector Cruz, Angela Cruz, Carolina Cruz, and Natalia Cruz, my great supporters, for encouraging me, believing in me, and looking out for me even as I away for graduate school. My mother, whom I love, I thank. You have been a great friend and encourager, and I thank God for you. To my dad, thank you for your words of encouragement. To Angela, for your friendship and love. To Carolina, for your affection and love. And Natalia, my youngest sister, for your love and support. I look forward to seeing you soon.

I also would like to acknowledge my friends in Florida Feraaz Hosein, Trenton Barrick, Grant Lewis, Woody Joseph, Josue Torrens and the Harbour Church. I also would like to thank all my friends from the Justice House of Prayer in Boston and Hilltop Church, whom have been a comfort to me. Also to Eder and Nando Teixeira, my roommates Neil Guram, and Thabang Nare, Kaleb Goodwin, and my friends Kevin and Josephine Bagnall, and to all from Christians on Campus, thank you for your friendship. And to everyone whom has kept up with me, at MIT or outside, and has been a friend to me during my time in graduate school, thank you!

Samuel Cruz

## List of Figures

**Figure 1** | HRXRD omega/2theta coupled scan of GaN grown on epitaxial graphene synthesized on a SiC (0001) substrate .....pg. 20

**Figure 2** | HRXRD omega/2theta coupled scan of GaN grown on LRGT exfoliated graphene transferred onto a 300nm SiO2 layer thermally grown on an (Si 001) substrate ..... pg. 21

**Figure 3** | Results of DFT simulation of planar averaged electron density with a varying separation gap .....pg. 23

**Figure 4** | Results of DFT simulation of planar averaged electron density with a varying separation gap .....pg. 24

**Figure 5** | Model for DFT natural separation distance calculations .....pg. 25

**Figure 6** | Results of graphene layer stacking experiment on epitaxial orientation of overlayers .....pg. 28

**Figure 7** | Results of epitaxial monolayer graphene experiment on orientation of GaAs overlayer .....pg. 30

**Figure 8** | High resolution STEM images of GaAs on graphene on GaAs (100).....pg. 31

**Figure 9** | InP and GaP growths on epitaxial graphene transferred onto (001) InP and (001) GaP substrates.....pg. 32

# Chapter 1

## Mechanism of Remote Epitaxy using Two Dimensional Materials

### Background

#### The “long range” effect

Experiments by Distler in 1968 show that evaporating Ag on a (010) cleaved surface of a Triglycine Sulfate (TGS) crystal lead to the nucleation of Ag in clearly discernible patterns on the substrate surface (2). This was known as a “decoration” method and was used to infer properties of surface potential (3, 4). The deposition here happened at low substrate temperatures, in the order of 20 C. From this work the claim was made that nucleation was favorable at “active” sites on the substrate surface, that is, the sites where the Ag was observed to prefer to nucleate. Depositing at higher temperatures got rid of the nucleation patterns to where nucleation was then observed to be uniform on the surface. Thus, it distorted these “active” sites where nucleation first took place to “decorate” the surface and give information about where the deposited material preferred to nucleate (3).

In his 1969 Nature paper (5), Distler and Shenyavskaya report that amorphous interlayers in epitaxy could act as conduits for the transfer of the structural information required to direct epitaxy, where the overlayer was oriented by the underlying single crystal substrate. It was proposed that the structural information which allowed this originated from the strong potential at charged “defects” on the surface of the single crystal substrate, which could induce a micro-electret



polarization in the amorphous layers. This polarization on the amorphous layer could help direct epitaxial growth in resemblance of the underlying substrate provided the layer was below a critical thickness. In trying to figure out this mechanism, they explored the question whether the amorphous interlayer was transferring the structural information by acting simply as an inert spacer, or if it was providing the structural information through a mechanism in which the structural information was embedded in it by the single crystal substrate. Experiments were run to determine if single crystal substrates could embed electrical polarization information from the strong potential at the charged defects into the amorphous layers. Results demonstrated that the orienting mechanism depended on the electrical potential shape at the surface of each substrate. For example, growing AgCl on the surface of silicon by thermal evaporation under vacuum of  $\sim 10^{-5}$  Torr on amorphous carbon ( $\sim 10$ -80nm) deposited on the surface of a silicon single crystal with a p-n junction on its surface, demonstrated that AgCl could achieve a single crystal orientation on the p- doped region on the surface, whereas the n- doped region of the surface yielded polycrystalline growth.

Moreover, AgCl growth on the released side of the amorphous carbon removed from the single crystal substrate yielded the same selective crystallization result that was obtained as when the amorphous carbon layer was on the single crystal substrate. This was termed the “memory” of interfacial films. The authors perceived to explain this mechanism by postulating that the amorphous films had a “memory” which was embedded by the substrate via internal electret polarization of the amorphous carbon film (5). This polarization of the amorphous layer could help direct epitaxial growth in resemblance of the underlying substrate provided again that the layer was below a critical thickness.

Other works on crystal growth with an amorphous interlayer followed. Another study reports on the growth of AgCl on directly on a TGS crystal with and without a thin amorphous Se interlayer on its surface. The same nucleation pattern and orientation was observed both directly on the TGS surface and on the deposited amorphous layer on TGS, provided the amorphous layer was below a critical thickness. Through this came what was described at the time as the “long range effect” of a single crystal substrate (3), following the previous observations where the “electrical nature” of the substrate crystal “matrix” (periodic arrangement of atoms in space) created a “linear” potential that would extend to influence the deposited overlayer beyond a thin amorphous or polycrystalline interlayer below a critical thickness. Experiments to extend this theory included growth on a variety of other crystalline materials (4, 6). For example, the growth of CdS through amorphous SiO and carbon, ranging in thickness from 7 to 15 nm using Mica as a substrate, yielded single crystal layers aligning crystallographically with the substrate, given the amorphous layers were less than 12nm for SiO and 10nm for Carbon (4). In short, the substrate could provide the necessary information to orient an overlayer through an amorphous interlayer if it were below a critical thickness. If this critical thickness were exceeded, the amorphous layer would filter out the defect sites thought to be required to orient overlayers, which hindered oriented crystallization (6).

These results did not come without constructive criticism. Near the time of these claims, a theory was not proposed for this epitaxy mechanism, but rather just a postulate of physics the mechanism itself (7). The results were controversial at the time given the common knowledge that epitaxy was not possible on purely amorphous substrates, and the postulation that if this were

deposited on the single crystal substrate, it would destroy any epitaxial relation. Or also the implausibility that the substrate could transmit any electrical information through tens to hundreds of angstroms of an amorphous coating. Critics of this work proposed the possibility that the amorphous carbon coating was not uniform and thus epitaxial growth proceeded by lateral growth through porous sites on the substrate which were not covered. In addition, the conductive nature of amorphous carbon made it less likely that directed charge effects could be transmitted through its thickness (7). However, these negative results, along with those from Distler, were later confirmed (8).

Further, Tsu in 1998 also reports on the epitaxial growth of silicon through a disordered layer of oxygen introduced in a controlled quantity to cover the Si surface. The buffer growth of a Si layer here is followed by the introduction of oxygen into the chamber in the aim of achieving the following structure: one monolayer of oxygen on a silicon surface, followed by epitaxial growth of 1.1nm of Si, followed by another oxygen layer, and finally more silicon. The proposed mechanisms for obtaining epitaxial silicon with oxygen at the surface is that the surface may not have been fully covered with oxygen, and thus lateral growth could occur. The other explanation is that the layer of oxygen (~monolayer) at the interface is in a strained state, and the surface potential of the silicon may not be totally obscured by it (9). This latter explanation supports the claim of the so called “long range effect” (3).

Such studies represent some of the background regarding the “long range effect” through amorphous layers. In our case, we would like to utilize such knowledge to advance and develop van der Waals epitaxy (vdWE) through two dimensional materials and advance the thin film

fabrication technique which the research group of the author of this work have termed the “two-dimensional material based layer transfer” (2DLT) technique for a variety of applications including solid-state lighting, photonics, photovoltaics, and their flexible counterparts.

### **The advent of van der Waals epitaxy**

Van der Waals epitaxy was initially conceived through the growth of materials with inherent van der Waals (vdW) cleavage planes in their crystal structures—vdW solids—where high quality growth of single crystal films proceeded at an atomically sharp vdW interface. The main characteristic of the vdW surface is that it has no broken bonds. This allowed the heteroepitaxial growth of layered materials with different lattice constants and even different crystal structures by relaxing the lattice matching condition at the surface required in conventional epitaxial growth (10–12). This was believed to be facilitated given that epitaxial growth proceeded on a surface free of dangling bonds via the weak vdW forces inherent to the layered material, as opposed to the much stronger direct covalent or ionic binding of crystals, where surface dangling bonds make direct and strong covalent or ionic binding to adatoms (13). The concept attempted to address the limitation that device heterostructures could only be achieved with select semiconductors that had such close lattice match as to prevent defects from forming, such as dislocations, which precisely arise from lattice mismatch at the growth interfaces of covalently or ionically bonded crystals (10, 11). However, while most focus was centered on the weak van der Waals binding mechanism at the surface of the substrate—which was believed to allow the single crystal film formation despite large lattice mismatch by relaxing the binding forces (12)—less attention was placed to the role of the bulk substrate underneath the immediate surface, and its

effect on the formation of such layers. Thus, van der Waals epitaxy as originally conceived essentially comprises a van der Waals surface to allow relaxation of the lattice matching condition at the interface to grow a single crystal film. This means that epitaxial growth using the van der Waals surface mechanism could essentially proceed if one had a single crystal surface whose surface dangling bonds are passivated. Moreover, the fact that vdW layered solids are easy to cleave given their vdW bonding nature, also allows for the exfoliation of the growth material after epitaxial growth. This material can then be transferred to a desired surface and novel devices can be designed, taking advantage of the geometry of thin film of many materials. Also, the flexibility of exfoliated thin films from a surface allows the design of novel electronic devices.

### **The emergence of graphene and 2D materials**

The advent of graphene and its outstanding properties render it potentially useful and a game changer in a plethora of technologies, including novel high speed electronics (14). As such, much effort has been devoted to synthesizing and characterizing high quality graphene. Given its outstanding electrical conductivity, graphene has been considered as a candidate to make high speed transistors, though with limited success given the difficulty to create a bandgap in graphene, hindering its adaption as an electrical switch. However, the outstanding properties of graphene lend its use for a variety of other applications. Graphene is a 2D materials with a hexagonally arranged  $sp^2$  bonded carbon atoms. It is an atomically thin, flexible, and strong material. It is also the building block for three-dimensional graphite. Its layered configuration in graphite is characterized by weak vdW forces at the cleavage planes. Thus, graphene is a vdW material. Its 2D vdW crystalline material nature, along with its mechanical, chemical, and electrical properties

have rendered graphene a candidate to perform vdWE of 2D and 3D crystals (15–22). Since its discovery, there have been numerous methods to synthesize graphene, including exfoliation, and by using carbon precursors in the gaseous phase by chemical vapor deposition (CVD). While its initial isolation upon its discovery was using micro-meter sized flakes, graphene can now be synthesized as a monolayer—or isolated to a monolayer—at large scale using Cu foil, (0001) SiC, and (100) (110) and (111) Ge substrates, among other substrates (23–25). The van der Waals surface of graphene may also be used to passivate the surface dangling bonds to achieve vdWE-like growths like those on bulk vdW solids, hence allowing the possibility of performing vdWE on any surface to which the vdW 2D material can be transferred. Thus, 2D materials can now become useful components in the advancement of vdWE for the growth and transfer of 2D and 3D crystals.

### **Orienting contributions from the underlying substrates in vdWE using 2D materials**

More recently, the single crystalline growth of semiconductor materials has been attempted on the vdW surfaces provided by 2D materials such as graphene (22, 26–29) and hBN (30), where the weak vdW out of plane binding interactions of these materials—as opposed to covalent or ionic—make them attractive as release layers (19, 31, 32). Such 2D materials were either grown or transferred on arbitrary substrates (15, 16, 19, 20, 28, 32–34). However, the notion in some of these works is that the 2D layered material is the sole provider of the seed for epitaxial growth in vdWE. However, the substrate underneath the grown or transferred 2D material may still play a role in the mechanism of orienting surface adatoms in vdWE to form an epilayer. This is because the potential from the substrate may be so strong as to overpower the

much weaker potential field of atomically thin 2D materials. This is suggested to us by the observed “wetting transparency” of graphene (35–38).

Specifically, experimental and theoretical water contact angle studies on the on the surface of graphene (35–37) suggest that the substrate may have a significant effect on the growth of an overlayer. For example, the contact angle of static water droplets on a material surface are a measure of the wettability of a solid surface as well as degree of molecular interactions. It has been reported that the presence of graphene did not affect the contact angle of water droplets on selected substrates—whose surface interactions were not dominated by chemical bonding—and thus here, graphene acted as “transparent” (35). However, it was later found that the contact angle is significantly affected by the presence of monolayer graphene, except for surfaces with moderate contact angles ranging from around 40 to 90 degrees, where the graphene acts only as semi-transparent (36). A later study reported that the roughness of the surface and various wetting modes should be considered to better interpret the varying contact angle measurements observed with graphene, and that the substrate effect becomes negligible with as few as two stacked graphene layers (37). Thus, monolayer graphene may be “semitransparent” to the substrate, meaning the substrate has a substantial effect on the contact angle of the overlaying water droplet. Thus, if polar water molecules are affected by the underlying substrates, so too may be the case with overlayers during epitaxial growth attempts on graphene.

## **Our use of graphene**

Since its discovery, research on graphene has moved at a fast pace. As such, key developments such as the ability to fabricate it at large scales make it attractive to perform vdWE

of 3D semiconductors of technological importance. The main aspects of graphene that may be utilized for vdWE type growths is its extreme thinness. At only one atom thick, graphene allows perhaps the closest achievable distance between substrate and overlayer when it acts as interlayer. Thus, the probability of the underlying substrate—with its electrical surface potential— influencing epitaxial growth, increases. Next, as aforementioned, the vdW surface would allow separation of grown layers at graphene. This is of great technological importance given that producing thin films of exotic semiconductor materials such as SiC, GaN and GaAs, cheaply, may allow tremendous substrate cost savings, and allows for new applications such as flexible electronics of many materials, and characterization of new physics. This thesis, will, however, focus on the mechanism of vdWE on graphene via what has been termed “remote epitaxy” (1).

### **Gallium Nitride epitaxy on graphene**

Graphene has been explored as a seed to grow GaN films by many researchers since the hexagonal graphene lattice resembles the hexagonal c-plane of GaN (17, 19, 22, 26, 28, 29, 32, 39). Different types of graphene such as flakes, polycrystalline graphene, and epitaxial graphene have been explored as a seed layer for growing GaN films (17, 19, 22, 26, 28, 29, 32, 39). Among those, single-crystalline GaN has been achieved on epitaxial graphene grown on SiC substrates (19). Obtaining single-crystalline GaN on graphene permits the development of a two-dimensional material based layer transfer (2DLT) technique, where single-crystalline GaN epilayers are released precisely from the surface of graphene and the graphene substrate is reused multiple times without any refurbishing step (19). It has been believed that this accomplishment is owed to the unique orientation of epitaxial graphene grown on the SiC substrate, which serves as the seed layer



that promotes single crystalline epilayer formation. However, the underlying SiC substrate below graphene may still play a role in determining orientation of epitaxial overlayers because the epilayer-substrate distance is atomically small. This hypothesis is supported by literature on the effect of the strong substrate surface potential.

## **Research objectives**

The objectives of this research are to clarify the contribution of graphene as a seed layer, and the effect of the underlying substrate on the crystallographic orientation of overlayers. As such, we undertake extensive experimental methods to characterize crystallinity, epitaxial alignment, morphology of grown layers, and exfoliation of layers. Methods utilized for this purpose include High Resolution X-Ray (HRXRD), Scanning electron microscopy (SEM), Transmission electron microscopy (TEM), and Electron Backscatter Diffraction (EBSD) of overlayers. In this work, we find that the substrate has a significant orienting effect during epitaxial growth, and that a single sheet of graphene may allow for the transfer of crystallographic information through its single-atomic thickness to orient overlayers in epitaxy. This ability has been termed “remote epitaxy” (*1*).

This page is intentionally left blank

# Chapter 2

## Epitaxial growth through graphene

### Role of the underlying substrate in GaN/graphene/SiC system

As discussed in the introduction, the literature seems to suggest that the 2D material, graphene in this case, has been considered as the seed layer in vdW epitaxy (17). This is not surprising given that in some of these works, GaN was the semiconductor crystal being grown. The hexagonal resemblance of the c-plane of hexagonal close packed (hcp) single crystals and graphene are plausible to support these claims. Further, when growing GaN on graphene on SiC, graphene is synthesized by the sublimation of silicon at very high temperatures. Given that carbon atoms can rearrange on top of the SiC surface to form graphene, the seed layer of vdWE of GaN on this type of graphene may be even more difficult to discern, given that the hcp SiC (0001) substrate and graphene are epitaxially aligned (19). Figure 1a shows a schematic of the growth structure. An HRXRD coupled  $\omega/2\theta$  scan is shown in Figure 2b, demonstrating single crystallinity of (0001) wurzite GaN grown on epitaxial graphene on SiC (0001). The single-crystallinity of this GaN epilayer was well proven in a previous work by electron backscattered diffraction (EBSD) mapping and STEM (7). The epitaxial growth of GaN in this work was conducted using a Molecular Beam Epitaxy (MBE) system.

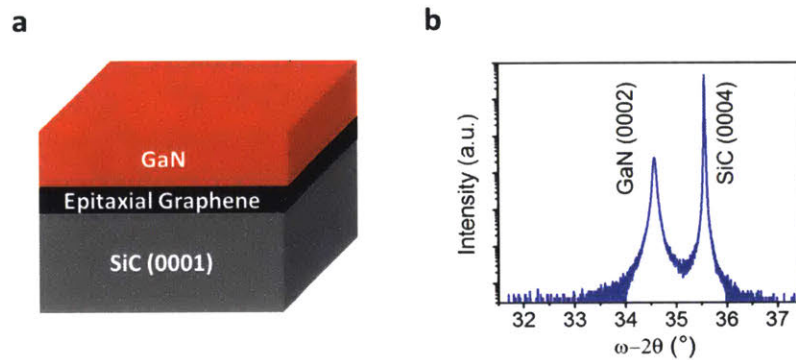


**Figure 1 | HRXRD omega/2theta coupled scan of GaN grown on epitaxial graphene synthesized on a SiC (0001) substrate a, Schematic showing the heteroepitaxial structure b, HRXRD showing single crystallinity of the GaN epilayer when grown on SiC (0001).**

We turn to break the relationship between graphene and its underlying SiC substrate to determine whether graphene or SiC is the seed. To do this, we resort to using a layer-resolved graphene transfer (LRGT) method (24) to remove graphene from the surface of SiC, and transfer it to our substrate of choice for this study (19). As a first step to investigate the role of the substrate as a seed in the vdW epitaxial growth of GaN on SiC, we transfer graphene onto an amorphous 300nm thick SiO<sub>2</sub> layer thermally grown on a Si (100) substrate. Due to the amorphous nature of SiO<sub>2</sub>, the only potential single-crystalline seed is expected to stem from the epitaxial graphene monolayer. We perform the growth of GaN by MBE. An omega-2theta HRXRD coupled scan of this sample revealed that a GaN film grown on graphene/SiO<sub>2</sub> is polycrystalline (Fig. 2b), implying that the substrate below the graphene layer plays a role in determining the epitaxial orientation of the GaN films. The result also implies that, given GaN and SiC have the same hcp crystal structure coupled with a small lattice mismatch, this could be the factor that allows single-crystalline GaN formation through graphene on the SiC substrate surface.

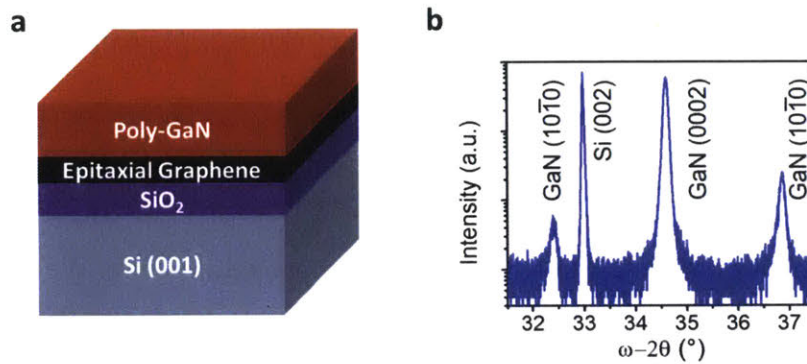


**Figure 2 | HRXRD omega/2theta coupled scan of GaN grown on LRGT exfoliated graphene transferred onto a 300nm SiO<sub>2</sub> layer thermally grown on an (Si 001) substrate. a**, Schematic showing the heteroepitaxial structure **b**, HRXRD showing polycrystallinity of the GaN overlayer when grown on an epitaxial graphene/SiO<sub>2</sub>/Si (001) substrate.

Moreover, this finding led us to explore the possibility of performing remote epitaxy through a graphene interlayer. This can be realized if the crystallographic information from the substrate can be transferred to the overlayer through graphene to orient adatoms. The implications of this idea are great. For example, vdWE can relax the growth and lattice matching between materials. Thus, epitaxy through 2D materials could may allow the relaxation of the lattice matching condition, and since the interface bonding is weak, there is less probability to nucleate defects and dislocations (*I*). Moreover, the vdW surface would allow exfoliation of functional as-grown films.

### Density functional theory simulations

The effect of the substrate—based on the previous finding of the substrate effect on the growth of GaN on graphene grown on SiC (0001)—is further explored. Density Functional Theory

(DFT) simulations are implemented to calculate the extent of interaction of an overlaying layer with a substrate through graphene. To approximate this, we first model the interaction between slabs representing substrate and epilayer, and calculate the averaged planar electron density interaction as the gap between them is varied from 5 Å and 30 Å. However, we consider epitaxial growth through graphene onto a substrate with a different crystal structure. We choose GaAs (100) as a substrate material to conduct this study because of the crystallographic contrast between the hexagonal graphene lattice and hcp wurzite GaN to the cubic zinc-blende crystal structure of a GaAs (001) substrate. The computations were done using the plane-wave pseudopotential code Quantum Espresso (40). The Perdew-Burke-Ernzerhof general gradient approximation was utilized for the local exchange correlation (41). All atoms during the simulation were relaxed.

One of the main differences in this case is that we rather attempt homoepitaxial growths through graphene on GaAs (001). Figure 1a shows the substrate epilayer slab model for As-terminated and Ga-initiated slabs, representing substrate and epilayer, respectively. GaAs wafers usually come with an As-terminated surface. Thus, we account for As- or Ga- initiation if a growth were performed by inserting a graphene interlayer. The planar averaged electron density interaction for this configuration yields a critical distance—beyond which interaction is lost—of approximately  $\sim 9$  Å.

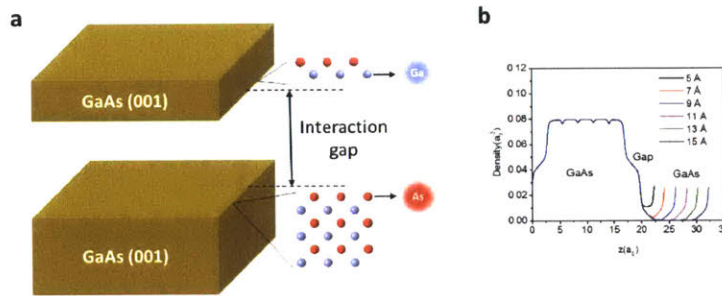


**Figure 3 | Results of DFT simulation of planar averaged electron density with a varying separation gap. a**, Schematic demonstrating the model, and showing the termination at the surface which was accounted for, in this case, As- termination and Ga- initiation **b**, planar averaged electron density interaction as a function of separation distance between slabs, showing the cutoff distance to interaction is  $\sim 9 \text{ \AA}$  and no interaction between the slabs is expected after this point.

Similarly, Figure 4b shows a schematic of the slabs, except now with As-termination and As-initiation in the slabs. As in the previous case, the critical interaction distance after which planar averaged electron density interaction is lost is also around  $\sim 9 \text{ \AA}$ . Thus, around a  $\sim 9 \text{ \AA}$  separation gap or beyond, no interaction should be expected and epitaxial growth cannot happen. Alternatively, bringing the slabs as close together as possible yields strong electron density interaction, signifying crystal binding can occur.

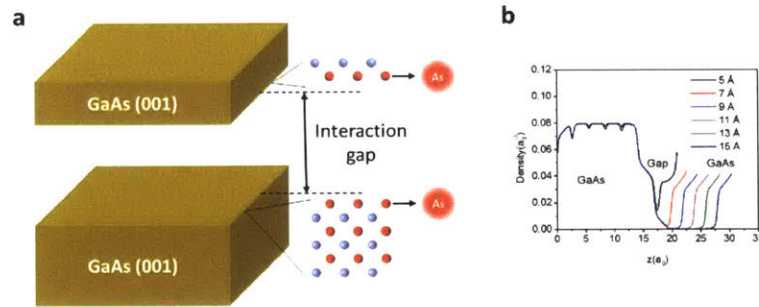


**Figure 4 | Results of DFT simulation of planar averaged electron density with a varying separation gap. a**, Schematic demonstrating the model, and showing the termination at the surface which was accounted for, in this case, As- termination and As- initiation **b**, planar averaged electron density interaction as a function of separation distance between slabs, and like Fig. 3b, the interaction distance cutoff is around  $\sim 9$  Å.

Having found a critical interaction distance between the slabs of  $\sim 9$  Å, we now turn to the question of performing epitaxial growth remotely through interlayer graphene. The theoretical natural interlayer spacing in graphite is taken to be 3.3 Å. We next compute the number of layers of graphene that can be inserted in the 9 Å gap which may still allow remote interaction. To do this, two slabs separated by a graphene layer are modeled. One of the slabs and the graphene layer are then relaxed in the normal to the surface direction, and allowed to relax. After relaxation of all layers, the inter-layer spacing's were used to calculate the expected natural separation between GaAs slabs sandwiching an arbitrary number of graphene multilayers. Relaxation calculations were set to complete when the forces on the relaxed layers were less than  $10^{-3}$  a.u. Figure 5 shows the model implemented for each slab surface atom termination, with additional graphene layers inserted using the natural vdW spacing of graphite, 3.3 Å.



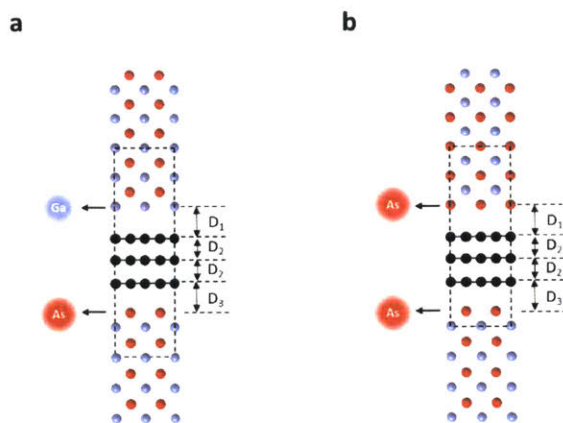


**Figure 5 | Model for DFT natural separation distance calculations. a**, Schematic demonstrating the model for As- termination and Ga- initiation and, **b**, As- termination and As- initiation through carbon layers.

The number of graphene layers that can be inserted in each configuration, that is, for As- and Ga-, versus As- As- surface atom configurations, is different due to the interaction of the carbon layer with each atom. We use the relation

$$D_{sep} = D_1 + D_3 + (n - 1)D_2 \quad (1)$$

to calculate the number of graphene layers that can be inserted in the  $9\text{\AA}$  critical interaction gap. Here  $D_{sep}$  represents the separation between each slab after insertion of  $n$  number of graphene layers. For Ga- and As- terminations (Figure 5a),  $D_1$ , the natural separation between the Ga-termination and the carbon layer is  $1.90\text{\AA}$ . Similarly,  $D_2$  represents the natural separation distance between the As- termination and the carbon layer, with  $3.14\text{\AA}$ . The total number of graphene layers that  $9\text{\AA}$  can accommodate with As- Ga- surface terminations is 2, with a total calculated distance of  $8.19\text{\AA}$ . Likewise, we compute the same distance except with As- surface terminations on both slabs (Figure 5b). Here,  $D_1 = D_2$ , since As- interacts with the carbon layer from both sides. The total number of layers that can be inserted in this case is only one, with a total separation of

6.28 Å. Thus, remote epitaxy may be possible with a monolayer graphene for As-As- surface terminations, and bilayer graphene for As-Ga- surface terminations. However, interaction between GaAs slabs may be dampened by the vertical van der Waal force exerted by interlayer graphene, although it is of an order of magnitude weaker than that of covalent interaction. Thus, the true charge interaction gap between the substrate and epilayer through which crystallographic information can be transferred may be less than that estimated by DFT simulations. Whether graphene can achieve remote interaction with these number of graphene layers is discussed with experimental regard in the next section.

### **Experimental trials of remote epitaxy**

To experimentally verify the possibility of obtaining remote interaction through graphene with GaAs (001), we resort to a series of studies involving the transfer of graphene onto GaAs (001) substrates. Monolayer, bilayer, and tetra-layers of graphene grown on Cu foils were transferred onto GaAs (001) using a Polymethylmethacrylate (PMMA) based wet transfer method (42). The Cu foil multi-layer transfer method was well developed by our collaborators. Epitaxial growth for this experiment proceeded via the use of a Thomas Swan close-coupled shower head Metal-Organic Chemical Vapor Deposition (MOCVD) reactor. Epitaxial growth of pristine epitaxial wafers is a very delicate process and contamination must be avoided to the greatest extent possible. Moreover, given that graphene does not diffuse into substrates at high temperatures, and thus acts as a diffusion barrier (43, 44) and impermeable surface, care must be taken to clean the GaAs substrate surface to remove the native oxide, which can hamper epitaxial growth. Thus, 10% dilute hydrochloric acid (HCl) solution in de-ionized (DI) water is used to treat the GaAs surface

prior to graphene transfer to clean the surface and strip its native oxide. Graphene is immediately transferred after this step. Given that this part of the experiment utilizes a wet transfer method, all samples were annealed at 350 °C in H<sub>2</sub> ambient to remove process residues at the interface and induce adhesion to the underlying substrate.

Next, the epitaxial growth of GaAs on all substrates is conducted. The precursors used for Ga and As are Trimethyl Gallium (TMGa) and Arsine (AsH<sub>3</sub>), respectively. The growth proceeds via a two-step growth. First, growth is set at a low temperature of 450 °C to promote nucleation on the graphene surface. This is followed by a conventional MOCVD GaAs growth step at a higher temperature, 650 °C. All growths occur at a pressure of 100 Torr. After growth, the grown film is exfoliated from the surface of the substrate utilizing a metal-stressor (19). The metal stressor acts to induce a stress in the film and at the film-graphene interface to promote and allow exfoliation of overlayers. Around ~100 nm of thermally evaporated Ti are deposited on each as-grown sample. Next, a high stress Ni layer is deposited using DC sputtering from a Ni target. Finally, a thermal release tape is applied to the heterostructure and an exfoliation act is performed, and fast release of the films is achieved.

Given that the films can be exfoliated from an atomically flat graphene vdW surface, this permits the use of Electron Backscatter Diffraction (EBSD) mapping to investigate the crystallographic orientation of the overlaying films. Figure 6 shows the results for growth on bilayer and tetra layer graphene.

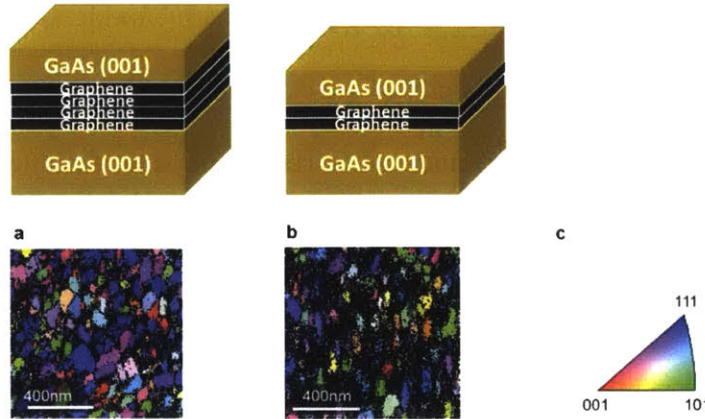


**Figure 6 | Results of graphene layer stacking experiment on epitaxial orientation of overlayers.** **a**, Schematic of the structure showing four layers of graphene transferred onto GaAs (001) (top), and EBSD mapping of the released side of the overlayer using tetra-layer stacks of graphene (bottom) showing that the substrate is not able to orient the overlayer, and this polycrystalline growth results. **b**, Schematic of the structure showing two layers of graphene transferred onto GaAs (001) (top), and an equivalent EBSD mapping of the released side of the overlayer using bilayer graphene (bottom), also yields polycrystalline growth, **c**, Inverse pole figure color legend indicating crystallographic orientation.

Next, we consider monolayer graphene. Upon using the graphene wet transfer method with Cu foils using PMMA, graphene meets Cu etchant solutions, such as Iron III Chloride ( $\text{FeCl}_3$ ), and other liquids, such as DI water. As such, process residues can be found on the graphene surface and adsorbed at the interface between graphene and the substrate (18,19, 20-23). Thermal annealing helps remove process residues from the surface and promotes adhesion to the substrate (22, 24, 26). However, for our purposes, an LRGT method for monolayer graphene is more appropriate, given the dry transfer nature of the method, which avoids graphene meeting liquids.

Although orienting effects from the substrate were observed using monolayer graphene wet transferred from Cu foils, the growth was sensitive to the cleanliness of the transfer, with no interaction having been achieved for samples that were not annealed. Alternatively, because graphene grown on SiC (0001) is exfoliated from the pristine and clean surface of SiC, and subsequently transferred onto the substrate of interest, this graphene transfer is expected to be closer to the substrate over wet transfer methods. An EBSD scan of the underlying surface of the exfoliated layer using graphene exfoliated with LRGT confirms that the domain corresponds to GaAs (001) along the entire surface (Figure 7b). HRXRD scan confirms that the layer is of one orientation, GaAs (001), due to the presence of the GaAs (004) peak (Figure 7b). An off-axis phi scan of the exfoliated layer confirms that there are no azimuthal rotations in the layer, and thus it is single crystalline (Figure 7e). Thus, epitaxial growth remotely through graphene has been shown to be allowed with the presence of monolayer graphene only, but not with bilayer or tetra-layer graphene, as hinted to us by DFT calculations. Thus, graphene has been shown to be electrically penetrable enough to allow the surface potential of the underlying substrate to influence the crystallographic orientation of overlayers (1).

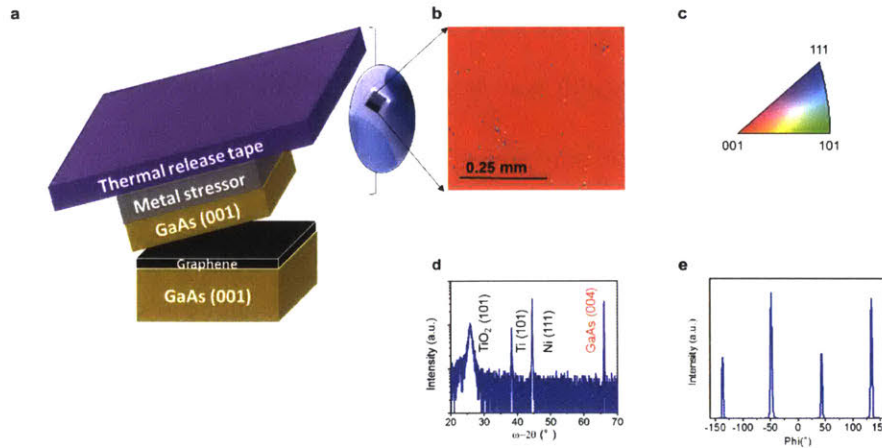


**Figure 7 | Results of epitaxial monolayer graphene experiment on orientation of GaAs overlayer.** **a**, Schematic of the structure showing the released overlayer/metal stessor/thermal release tape structure, **b**, EBSD map of GaAs grown on monolayer dry transfer graphene, showing that the layer is single crystalline 001 GaAs, **c**, Inverse pole figure color legend indicating the orientation of the EBSD scan, **d**, HRXRD scan of the underside of the exfoliated layer, showing that the layer is aligned crystallographically to the substrate, **e**, Off-axis  $\phi$  scan of the sample indicating that the layer is single crystalline without in-plane azimuthal rotations.

The epitaxial alignment between surface atoms of the substrate and those of the overlayer were resolved using Scanning Transmission Electron Microscopy (STEM). Figure 8a shows a STEM image (main) with convergent beam electron diffraction patterns showing the relationship between the (001) GaAs substrate (top) and the (001) oriented overlayer (bottom) are the same, which confirms their epitaxial relation. A measure of the natural separation distance is extracted from a STEM image, yielding  $\sim 5 \text{ \AA}$ , as shown in Figure 8c.

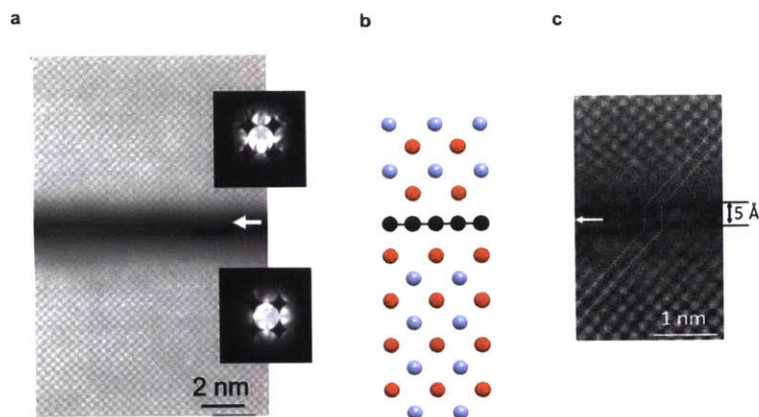


**Figure 8 | High resolution STEM images of GaAs on graphene on GaAs (100).** **a**, high resolution STEM image showing the epitaxial alignment through graphene. **b**, Schematic of the interface being imaged in STEM, **c**, STEM image with a measure of the natural separation distance.

### Probing remote epitaxy through other substrates

Remote epitaxy is further attempted on other substrates of interest and of materials which we have the capability of growing. As GaAs showed evidence of remote interaction through graphene, we turn to explore the effect of other substrates on homoepitaxy. Given that one monolayer allows remote interaction in GaAs, there is a high probability that it will allow the same on other substrates. Epitaxial graphene is transferred onto (001) InP and (001) GaP substrates following the LRGT method (24). Epitaxial growth of InP and GaP are conducted in MOCVD using TMGa, Trimethyl Indium (TMIn), and Phosphine ( $\text{PH}_3$ ) as precursors. Figure 9 shows the results of these experiments. Both InP and GaP are observed to grow with the same orientation through monolayer graphene. EBSD confirms this as the map contains only red along the scanned area of the underlying surface. This corresponds to 001 orientation for both GaP and InP (Figure 9 a and e). Moreover, HRXRD scans of the exfoliated layer confirm that the layer is epitaxially

aligned with the substrate in the 001 direction for both InP and GaP (Figure 9b and e). Both samples are exfoliated from their substrates. The flexible thin films are seen in Figure 9 c and f.

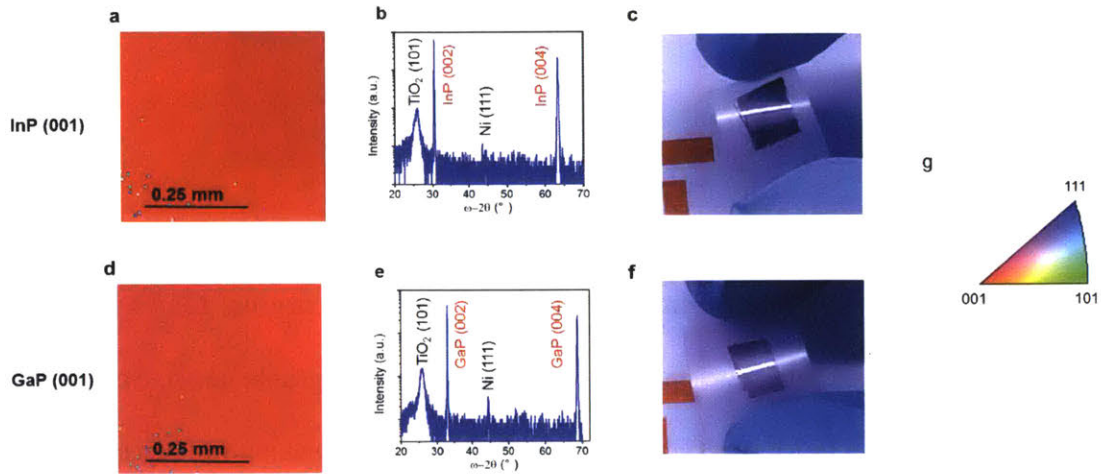


**Figure 9 | InP and GaP growths on epitaxial graphene transferred onto (001) InP and (001) GaP substrates. a**, EBSD map of a released film of InP grown on epitaxial graphene on (001) InP, showing one orientation in the overlayer, **b**, HRXRD of exfoliated layer confirming the layer is of one orientation. The InP (004) and the (002) double diffraction peak appear in the spectrum indicating (001) oriented InP, **c**, Image of exfoliated InP on thermal release tape, **d-f** EBSD and HRXRD of exfoliated layer, and image showing the exfoliated substrate. GaP is also observed to grow with the same crystal orientation as the substrate through graphene, **g**, Inverse pole figure color legend indicating crystallographic orientations.



## **Conclusion**

The work contained herein has shown that remote epitaxy is possible through monolayer graphene. This was explained by the interaction between graphene and the substrate. That is, for the substrate below graphene to orient the overlayer, it must be within the critical interaction gap calculated by DFT, otherwise, the distance is too far and no remote epitaxy may occur. Graphene is shown to be sufficiently thin and electrically penetrable to allow overlayers to be oriented through it by the underlying substrate. The natural separation distance of epilayer and substrate through monolayer graphene was shown to be smaller than the critical cutoff required to achieve interaction through graphene. For remote epitaxy attempts on bilayer and tetra-layer graphene, this distance is almost equal to or greater than the critical interaction gap. Thus, the greater separation does not allow these layers to be oriented by the substrate, and polycrystalline growth results. Moreover, the ability to exfoliate the grown overlayer is a great advantage to produce novel thin film devices for applications in advance electronics, photonics, and solar.

## **Future work**

Monolayer graphene has shown to be a key finding to be able to achieve interaction between epilayer and substrate during remote epitaxy through graphene. Notably, for the 2DLT method to become a universal method of thin film fabrication, the physics on interaction must be unveiled. We note that the successful growths on graphene so far have been performed on a limited range of materials. With the help of simulation methods, further material systems can be explored and predictions can be made to develop the 2DLT method. A universal method would allow the fabrication of functional thin films of all materials, which it has not been done in the past. To this

end, future work will focus on understanding the interaction between monolayer graphene and the materials that surround it during remote epitaxy. The plethora of properties of various crystals give rise to different interactions between graphene and each substrate during remote epitaxy. We propose to explore a range of crystals with characteristic ionic or covalent bonding, and elucidate the interaction of graphene with these materials and its effect on overlayer growths. Such research can lead the way to the full development of the 2DLT method for achieving functional thin films of high quality. So far, we have demonstrated the homoepitaxial growth of III-V polar crystals GaAs, InP, and GaP through graphene. Non-polar group IV crystals Si and Ge, along with other technologically relevant compound semiconductors such as GaN are under exploration, as they are systems upon whose interaction with graphene during remote epitaxy may yield valuable insight.

THIS PAGE IS INTENTIONALLY LEFT BLANK

## References

1. Y. Kim *et al.*, Remote epitaxy through graphene enables two-dimensional material-based layer transfer. *Nature*. **544**, 340–343 (2017).
2. A. R. Mattocks, © 1968 Nature Publishing Group. *Nature*. **217** (1968).
3. G. I. Distler, V. P. Vlasov, V. M. Kanevsky, Orientational and long range effects in epitaxy. **33**, 287–300 (1976).
4. A. V Kovda, L. L. Aksyonova, G. I. Distler, Y. M. Gerasimov, E. I. Kortukova, Growth of monocrystalline CdS films on mica through amorphous interfacial layers of silicon monoxide and carbon by chemical transport reactions. *Thin Solid Films*. **20**, 217–222 (1974).
5. B. Rosenburg, L. Van Camp, J. E. Trosko, V. H. Mansour, © 1969 Nature Publishing Group. *Nature*. **222**, 385–386 (1969).
6. G. I. Distler, a. N. Lobachev, V. P. Vlasov, O. K. Mel’Nikov, N. S. Triodina, Growth of single crystals through interfacial layers. *J. Cryst. Growth*. **26**, 21–26 (1974).
7. K. L. Chopra, Epitaxial growth of films on substrates coated with amorphous deposits. *J. Appl. Phys.* **40**, 906–907 (1969).
8. M. F. Perutz, 1970 Nature Publishing Group. *Nature*. **228**, 726–734 (1970).
9. R. Tsu, A. Filios, C. Lofgren, K. Dovidenko, C. G. Wang, Silicon Epitaxy on Si ( 100 ) with Adsorbed Oxygen. *Electrochem. Solid state Lett.* **1**, 80–82 (1998).
10. A. Koma, K. Sunouchi, T. Miyajima, Fabrication and characterization of heterostructures with subnanometer thickness. *Microelectron. Eng.* **2**, 129–136 (1984).

11. A. Koma, Summary Abstract: Fabrication of ultrathin heterostructures with van der Waals epitaxy. *J. Vac. Sci. Technol. B Microelectron. Nanom. Struct.* **3**, 724 (1985).
12. L. T. Vinh *et al.*, The van der Waals epitaxial growth of GaSe on Si(111). *J. Appl. Phys.* **81**, 7289 (1997).
13. K. Ueno, Epitaxial growth of transition metal dichalcogenides on cleaved faces of mica. *J. Vac. Sci. Technol. A Vacuum, Surfaces, Film.* **8**, 68 (1990).
14. A. K. Geim, K. S. Novoselov, The rise of graphene. *Nat. Mater.* **6**, 183–191 (2007).
15. Y. Alaskar *et al.*, Theoretical and experimental study of highly textured GaAs on silicon using a graphene buffer layer. **425**, 268–273 (2015).
16. Y. Zhang *et al.*, Direct observation of the transition from indirect to direct bandgap in atomically thin epitaxial MoSe<sub>2</sub>. *Nat. Nanotechnol.* **9**, 111–5 (2014).
17. Z. Y. Al Balushi *et al.*, The impact of graphene properties on GaN and AlN nucleation. *Surf. Sci.* **634**, 81–88 (2015).
18. Y. Alaskar *et al.*, Towards van der Waals Epitaxial Growth of GaAs on Si using a Graphene Buffer Layer. *Adv. Funct. Mater.* **24**, 6629–6638 (2014).
19. J. Kim *et al.*, Principle of direct van der Waals epitaxy of single-crystalline films on epitaxial graphene. *Nat. Commun.* **5**, 1–7 (2014).
20. Y. Shi *et al.*, van der Waals Epitaxy of MoS<sub>2</sub> Layers Using Graphene as Growth Templates. *Nano Lett.* **12**, 2784–2791 (2012).
21. J. A. Miwa *et al.*, Van der Waals Epitaxy of Two-Dimensional MoS<sub>2</sub>-Graphene Heterostructures in Ultrahigh Vacuum. *ACS Nano.* **9**, 6502–10 (2015).
22. K. Chung, S. In Park, H. Baek, J.-S. Chung, G.-C. Yi, High-quality GaN films grown on

- chemical vapor-deposited graphene films. *NPG Asia Mater.* **4**, e24 (2012).
23. X. Li *et al.*, Large-area synthesis of high-quality and uniform graphene films on copper foils. *Science (80-. )*. **324**, 1312–1314 (2009).
  24. J. Kim *et al.*, Layer-Resolved Graphene Transfer via Engineered Strain Layers. **833**, 833–837 (2014).
  25. J. Lee *et al.*, Wafer-Scale Growth of Single-Crystal Hydrogen-terminated Germanium. **3**.
  26. H. Yoo, K. Chung, S. In Park, M. Kim, G. C. Yi, Microstructural defects in GaN thin films grown on chemically vapor-deposited graphene layers. *Appl. Phys. Lett.* **102** (2013), doi:10.1063/1.4790385.
  27. J. W. Shon, J. Ohta, K. Ueno, A. Kobayashi, H. Fujioka, Fabrication of full-color InGaN-based light-emitting diodes on amorphous substrates by pulsed sputtering. *Sci. Rep.* **4**, 5325 (2014).
  28. P. Gupta *et al.*, MOVPE growth of semipolar III-nitride semiconductors on CVD graphene. *J. Cryst. Growth.* **372**, 105–108 (2013).
  29. J. W. Shon, J. Ohta, K. Ueno, A. Kobayashi, H. Fujioka, Structural properties of GaN films grown on multilayer graphene films by pulsed sputtering. *Appl. Phys. Express.* **7**, 5–8 (2014).
  30. Y. Kobayashi, K. Kumakura, T. Akasaka, T. Makimoto, Layered boron nitride as a release layer for. *Nature.* **484**, 223–227 (2012).
  31. Y. Kobayashi, K. Kumakura, T. Akasaka, H. Yamamoto, T. Makimoto, Layered boron nitride as a release layer for mechanical transfer of GaN-based devices. *2014 Silicon Nanoelectron. Work. SNW 2014.* **484**, 223–227 (2015).

32. K. Chung, C.-H. Lee, G.-C. Yi, Trasferable GaN Layers Grown on ZnO-Coated Graphene Layers for Optoelectronic Devices. *Science (80-. )*. **330**, 655–657 (2010).
33. P. Gehring, B. F. Gao, M. Burghard, K. Kern, Growth of high-mobility Bi<sub>2</sub>Te<sub>2</sub>Se nanoplatelets on hBN sheets by van der Waals epitaxy. *Nano Lett.* **12**, 5137–5142 (2012).
34. Y.-C. Lin *et al.*, Direct Synthesis of van der Waals Solids. *ACS Nano*. **8**, 3715–3723 (2014).
35. J. Rafiee *et al.*, Wetting transparency of graphene. *Nat. Mater.* **11**, 217–222 (2012).
36. C.-J. Shih, M. S. Strano, D. Blankschtein, Wetting translucency of graphene. *Nat. Mater.* **12**, 866–869 (2013).
37. D. Kim, N. M. Pugno, M. J. Buehler, S. Ryu, Solving the Controversy on the Wetting Transparency of Graphene. *Sci. Rep.* **5**, 15526 (2015).
38. R. Raj, S. C. Maroo, E. N. Wang, Wettability of graphene. *Nano Lett.* **13**, 1509–1515 (2013).
39. V. D. Wheeler *et al.*, Epitaxial Growth of III--Nitride/Graphene Heterostructures for Electronic Devices. **61003**, 2–6 (1882).
40. P. Giannozzi *et al.*, QUANTUM ESPRESSO: a modular and open-source software project for quantum simulations of materials. *J. Phys. Condens. Matter.* **21**, 395502 (2009).
41. J. P. Perdew, K. Burke, M. Ernzerhof, Generalized Gradient Approximation Made Simple. *Phys. Rev. Lett.* **77**, 3865–3868 (1996).
42. G. B. Barin *et al.*, Optimized graphene transfer: Influence of polymethylmethacrylate (PMMA) layer concentration and baking time on grapheme final performance. *Carbon N. Y.* **84**, 82–90 (2015).

43. J. Cho *et al.*, Atomic-Scale Investigation of Graphene Grown on Cu Foil and the Effects of Thermal Annealing, 3607–3613 (2011).
44. B. Kiraly *et al.*, Electronic and Mechanical Properties of Graphene-Germanium Interfaces Grown by Chemical Vapor Deposition. *Nano Lett.* **15**, 7414–7420 (2015).